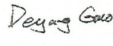
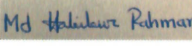



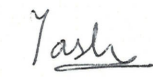


Strathclyde Engagement with the UK National HVDC Centre: Phase I Converter and GB Network Modelling

<i>Doc. Type:</i> Technical Report	<i>Date:</i> 12/09/2018	
<i>Doc. No:</i> USTRATH-HVDC Centre-P1-003	<i>Issue:</i> 3	<i>Page:</i> 1 of 30
<i>Title:</i> Offline DC grid model development		

	Name & Function	Signature	Date
<i>Prepared by:</i>	Deyang Guo, Md Habibur Rahman, Grain. P Adam, Abdullah Emhemed	   	10/09/2018
<i>Approved by:</i>	Lie Xu		12/09/2018
<i>Authorized by:</i>	Yash Audichya		

DISTRIBUTION LIST	N	A	I
Internal			
External			
N=Number of copy A=Application I=Information			


	Strathclyde Engagement with the UK National HVDC Centre: Phase I Converter and GB Network Modelling	<i>Doc. №:</i> USTRATH-HVDC Centre-P1-003
	Offline DC grid model development	<i>Issue:</i> 3 <i>Date:</i> 12/09/2018 <i>Page:</i> 2 <i>of</i> 30

TABLE OF CONTENT

1 INTRODUCTION 4

2 CONTROL METHODS OF DC GRID..... 4

2.1 CONVENTIONAL METHOD 5

2.2 MASTER-SLAVE CONTROL METHOD 5

2.3 DROOP METHOD 6

 2.3.1 Method 1 6

 2.3.2 Method 2 7

3 SYSTEM CONFIGURATION OF DC GRID 8

3.1 SYSTEM DESCRIPTION..... 8

3.2 WIND FARM CONFIGURATION..... 9

3.3 SYSTEM PARAMETERS 10

4 SIMULATIONS ASSESSMENTS OF THE DC GRID 11

4.1 CONVENTIONAL CONTROL METHOD 11

 4.1.1 Normal Steady-State Operation..... 11

 4.1.2 Symmetrical Three-phase AC Fault in the AC side of station MMC₁ 13

 4.1.3 Symmetrical three-phase AC fault in the AC side of station MMC₂ 16

 4.1.4 Symmetrical three-phase AC fault in the AC side of station MMC₃: 18

4.2 DROOP CONTROL-METHOD 1 20

 4.2.1 Normal Operation 20

 4.2.2 Symmetrical Three-phase AC fault at MMC₂ 22

4.3 DROOP CONTROL-METHOD 2 24

 4.3.1 Normal Operation 24

 4.3.2 Symmetrical Three-phase AC fault- fault at MMC₂..... 26

5 CONCLUSIONS 28

6 REFERENCES 29

Executive summary

To ensure supply reliability and economy of the power generated from various renewable sources multi-terminal DC grid is becoming one of the emerging solutions of future electricity network configuration. This report focuses on the DC grid configuration considering different control management effect on power flow of the grid. Moreover, this report provides a critical assessment of different control management, with emphasis on the capability and suitability of each method for a wide range of system studies such as AC side faults and network steady-state behaviour. A three-terminal half-bridge MMC based DC grid is developed in PSCAD platform for comprehensive studies and acting as the benchmark for the ongoing development and validation of real-time DC grid model in RSCAD platform. Simulations presented in this report reveal that grid management in terms of control assignment to its relevant converter station is the key factor. With proper control configuration of the grid, it enables normal steady-state operation as well as to continue transmitting limited power during any event of AC side fault.

1 Introduction

Increased global energy demands and high penetration of renewable energy generation will lead to new requirements for future electricity grids. There are increased needs for power exchange between neighbouring countries and power transmission over long distances. At present most of the HVDC links in operation connected between two points of a single AC system or two separate AC systems are commonly known as point-point HVDC links. Multi-terminal HVDC systems with more than two converter stations connected to the same DC network is an attractive alternative for future power grids due to the increased operational flexibility and reliability.

Line commutated converter (LCC) based HVDC is much more difficult to configure as DC grid due to the requirement to change the DC voltage polarity for power flow reversal. To change the DC voltage polarity can interrupt the entire power system. VSC technology has been the main focusing area of recent HVDC research due to its inherent advantages and will be the technology for future multi-terminal DC grid development. A number of pilot projects have been recently commissioned in China [1-3], though significant challenges exist for the manufacturers, network planners, and operators in DC grid development.

To balance the power flow within a DC grid, it is essential to assign at least one converter station to control the DC voltage of the grid. Ideally, no communication is required between the converters and the converters can be governed by their local controls and operate independently for the control of the DC grid [4-6]. Appropriate system control and protection must be in place to cope with abnormal conditions, e.g. during AC or DC faults.

The main objectives of this report are to develop a three-terminal DC grid associated with different control approaches for validating different operating condition. The developed PSCAD model and study presented will be used as a benchmark for the ongoing development of real-time DC grid model in RSCAD.

2 Control Methods of DC Grid

In DC grids, proper control of DC voltage is essential as any power imbalance within the DC grid will result in DC under/or over-voltages and affect DC grid stability.

Generally, it is important to restrict the variations of the DC voltage within a small range during both normal and abnormal operating conditions. Higher DC over-voltages increases stress on the DC cables, and converter semiconductors and passive devices, while DC under-voltages increase the system power losses and can potentially affect converters' ability to synthesize of the voltage imposed at their AC terminals by the AC grids. It is worth emphasizing that inability to synthesize the AC voltage poses the risk of loss of controllability. Therefore, it is mandatory to maintain a constant DC link voltage or allow DC voltage to be varied within a narrow range, with well-defined minimum and maximum limits for all operating conditions. Controlling the DC voltage of the DC grid in this way avoids most of the penalties that may arise as a result of major and sudden change in the operating condition (excessive over/under-voltages and transient power flows in the DC grid). Several control methods have been proposed for DC grids in the literature [7-12]. In this development, a few of these control methods are implemented and are highlighted below.

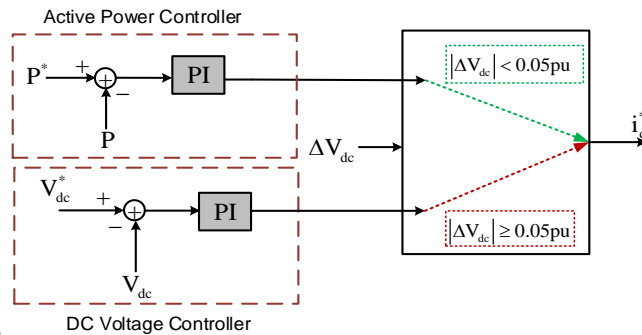
2.1 Conventional Method

In conventional point-to-point HVDC link, one converter station strictly regulates the DC voltage at a pre-set level, while the remaining terminal is designated to control active or DC power. This control method can be extended to a DC grid with multiple converter stations, with one converter station dedicated for controlling DC voltage at a particular level, while the remaining converters control their active powers at levels to be specified by the system operators. In this control method, the DC voltages of the power controlling converters will vary narrowly around that of the DC voltage controlling converter which acts as a power balancer (or DC slack bus) for the entire DC Grid. However, such a control method suffers from several drawbacks:

- A malfunction of the only DC voltage controlling converter may lead to large DC voltage variation potentially causing system collapse.
- The DC voltage controlling converter must be sufficiently large and connected to a strong AC grid capable of compensating any mismatch between AC and DC powers. This means the host AC grid must be capable of sourcing or sinking any power mismatch between AC and DC powers without creating significant frequency variations (over/under frequency).

2.2 Master-slave Control Method

A master-slave control method described in [10] was proposed to avoid the risks of the conventional control method highlighted in Section 2.1 by quick re-allocation of the DC voltage control function from the failed DC voltage controlling converter to a new converter that previously controls active power. In this way, the loss of system controllability and its consequences can be avoided [13-15]. A master-slave control



method is shown in

Fig. 1. However, switching of control modes (from active power to DC voltage) creates significant transients in the DC grid, and again the converter that would assume the function of DC voltage control must be sufficiently large (capable of sinking or sourcing any mismatch that may occur between AC and DC powers) and must be hosted by a strong AC grid.

It is worth emphasizing that with minor modifications, the master-slave control method can be used to facilitate orderly switching of successive power controlling converters to operate as DC voltage controllers when the converter stations originally designated as the DC voltage controllers hit their rated current. In this manner, the DC voltage control function can be shared between multiple converters.

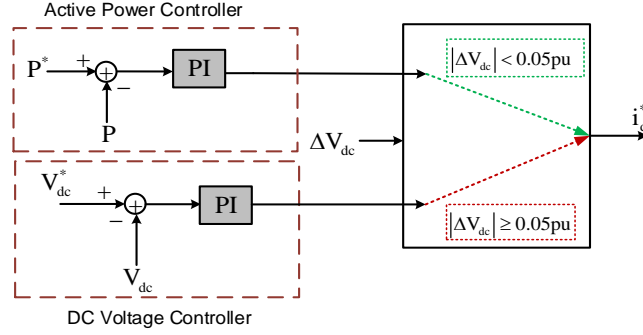


Fig. 1: Block diagram of a master-slave control

2.3 Droop Method

The traditional concept of droop control which is widely used to enable multiple synchronous generators to contribute to frequency control in AC power systems, has been adopted for controlling DC grids [9, 16, 17]. Droop control facilitates power control in DC grids that contain multiple converters, with or without specific converter dedicated for DC voltage control. Several studies have shown that droop controlled DC grids exhibit higher reliability during major system disturbances compared to the master-slave control and does not cause substantial over-voltages or transient power flows.

Amongst different types of droop control methods extensively studied in the literature, two types of droop control methods are elaborated in this report [18, 19].

2.3.1 Method 1

This implementation of droop control allows more than one converter to participate in DC voltage regulation of the DC grid at the same time, while the remaining converters control active power or execute any other control functions to be specified by the control centre. For an example, in case with two converters participating in DC voltage regulation, one converter terminal can strictly control DC voltage using a proportional-integral (PI) controller, while other can participate in DC voltage control through a droop (proportional gain) to provide less strict DC voltage regulation and facilitate power sharing between the connected AC grids. Fig. 2 shows an example of DC droop characteristic between DC current and voltage (Fig. 2(a)), and implementation of DC voltage-d axis current (active current) droop control (Fig. 2(b)). Mathematically, the droop characteristic shown in Fig. 2(a) can be expressed as:

$$I_{dc} = K_D(V_{dc} - V_{dc0}) \quad (1)$$

where K_D is the DC voltage-current droop constant and V_{dc0} reference point corresponding to zero Dc current (power). Assuming the converter of interest is lossless, the converter DC current I_{dc} can be approximated in term of direct d-axis AC voltage V_d and current I_d as:

$$I_{dc} = \frac{3}{2} \frac{V_d}{V_{dc}} I_d \quad (2)$$

After substituting (2) in (1), the following expression is obtained:

$$I_d = \frac{2}{3} K_D \frac{V_{dc}}{V_d} (V_{dc} - V_{dc0}) = K_T (V_{dc} - V_{dc0}) \quad (3)$$

where the droop constant is approximated by $K_T = \frac{2}{3} K_D V_{dc} / V_d$. Based on (3), the droop control in Fig. 2(b) is drawn.

Adoption of the droop control in Fig. 2(b) can improve DC grid controllability during AC fault scenarios by restricting the DC voltage variations within the predefined minimum and maximum limits. Therefore, this droop implementation can minimize the risk of total loss of system controllability, particularly, if the AC fault is sustained over a long period.

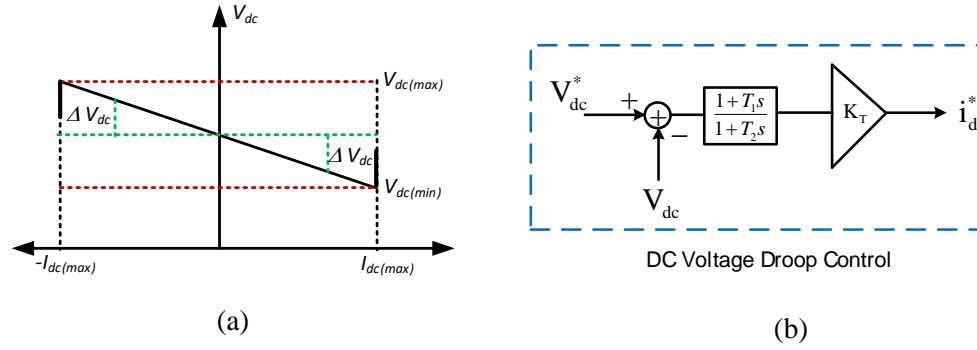


Fig. 2: Droop Method 1: (a) DC V-I droop characteristic (b) DC voltage droop control

2.3.2 Method 2

Besides the conventional DC voltage controlling converter that controls the DC voltage at constant values, the implementation in Fig. 3 (a) will enable the typical DC voltage controlling converters to exercise power control function. During normal operation, the P- V_{dc} droop will modify the original set-point of the DC voltage V_{dc}^* by ΔV_{dc} according to $V_{dc}^{**} = V_{dc}^* + \Delta V_{dc} = V_{dc}^* + K_p(P^* - P)$ in order to achieve the specified active power set-point P^* . Fig. 3 (b) depicts the P- V_{dc} droop characteristic implemented shown in Fig. 3 (a). As a large droop constant k_p is used, the actually power transmitted through the converter largely follows the set-point of P^* . When the output of the P- V_{dc} droop hits the maximum or minimum limits of the DC link voltage $\pm \Delta V_{dc(max)}$, the overall controllers in Fig. 3 (a) will act as DC voltage control with DC voltage set-point of $V_{dc}^* + \Delta V_{dc(max)}$ or $V_{dc}^* - \Delta V_{dc(max)}$, depending on the nature of AC and DC power mismatch (surplus or deficit). This scenario is more likely when the other main DC voltage controlling converter has failed or hit its maximum power limits. The typical value for $\Delta V_{dc(max)}$ could range from 2.5% to 5% depending on the detailed system design.

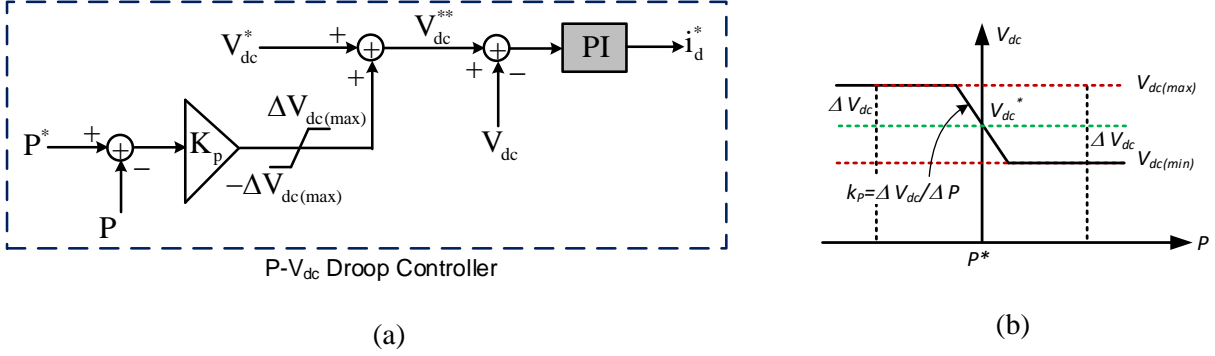


Fig. 3: Droop Method 2: (a) P-V_{dc} droop characteristic, (b) P-V_{dc} droop controller

3 System Configuration of DC Grid

3.1 System Description

Fig. 4 shows the developed three-terminal DC grid. Converter terminals MMC₁ and MMC₂ are connected to weak and strong AC grids with SCR=2.5 and SCR=15, respectively. The largest converter terminal MMC₂ which is connected to the strongest AC grid is the best candidate to operate as DC voltage controlling converter for the reasons stated earlier. Since MMC₃ is connected to a wind farm, MMC₁ could be controlled using one of the following models:

- Power control mode.
- Droop control method 1 to facilitate additional DC voltage control through the droop to provide less strict DC voltage regulation and facilitate power sharing between the connected AC grids.
- Droop control method 2 to embed power control function within MMC₁ and revert to DC control function when the main DC voltage controller is lost.

Converter terminal MMC₃ is controlled in islanding mode (grid forming converter) to establish AC voltage at the wind farm to absorb active power generated by the wind farm and to provide the required reactive power to the island network for ensuring constant AC voltage.

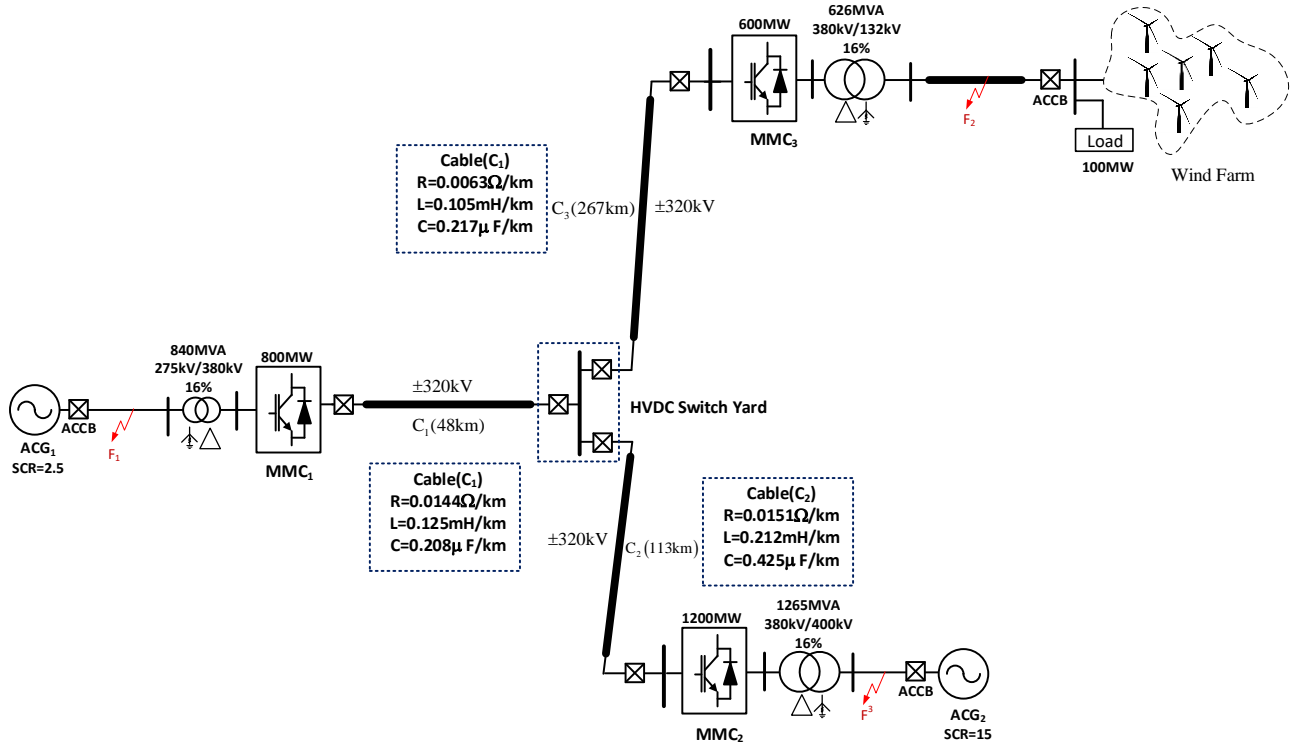


Fig. 4: Block diagram of a three-terminal MMC based DC grid

Detailed system parameters of the DC grid to be studied are shown in Fig. 4. The above discussions show that the allocations of control functions or modes to converter terminals depend on several factors such as:

- Strength of the host AC grid (strong or weak).
- Nature of the host AC grid or network (passive network with no established generation, e.g. wind farms).

For simulation efficiency, each converter in the DC grid shown in Fig. 4 is modelled in PSCAD by an averaged HB-MMC converter model explained and validated in reports 1 and 2. Each DC and AC cables are represented by a π -equivalent model.

3.2 Wind farm Configuration

The wind farm connected to MMC₃ is represented as an aggregated grid side converter model connected to a DC source as shown in Fig. 5. Thus, the detailed wind farm/turbine dynamics are not considered here as the purpose at this stage is to study the island network control by the MMC. The main controllers incorporated in the wind farm model are:

- Active and reactive power controllers
- Current controllers

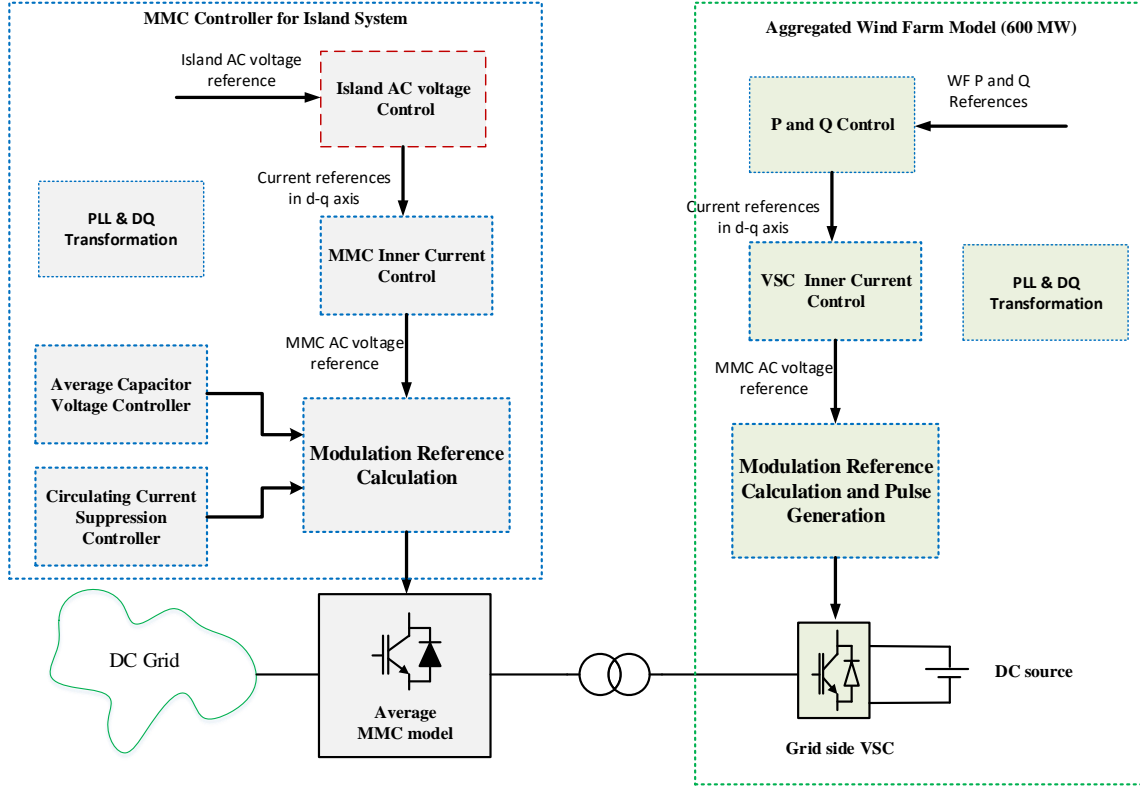


Fig. 5: An aggregated wind farm connected with MMC converter and control diagrams of the wind farm grid side converter and MMC converter

Fig. 5 shows the overall control structure of the wind farm grid side converter and MMC₃ converter. The MMC₃ that connects the wind farm to the DC grid adopts the same control systems detailed in reports 1 and 2 with the addition of outer AC voltage control loop. The wind farm converter controls its active and reactive powers according to the set-points.

3.3 System Parameters

The three MMC converters are interconnected through DC cables. The system parameters for the local AC grids, the wind farm, and MMC stations are given in Table 1, 2 and 3, respectively.

Table 1: System parameters (AC Side)

Item	Station 1	Station 2	Station 3
Rated Apparent Power (S)	840MVA	1265MVA	626MVA
Rated Active Power (P)	±800MW	±1200MW	±600MW
Converter Nominal DC Voltage	640kV (±320kV)	640kV (±320kV)	640kV (±320kV)
Converter Nominal AC voltage	380kV	380kV	380kV
AC Grid Voltage	275kV	400kV	132kV
Nominal Frequency	50Hz	50Hz	50Hz
SCR	2.5	15	-
X/R Ratio	10	10	10

Transformer rated Power	840MVA	1265MVA	626MVA
Transformer Voltage ratio	275/380kV	400/380kV	132/380kV
Transformer Reactance	0.16pu	0.16pu	0.16pu

Table 2: Wind farm System parameters

Item	Windfarm (WF)
Rated Apparent Power (S)	626MVA
Rated Active Power (P)	±600MW
Converter Nominal DC Voltage	1.2kV
Converter Nominal AC voltage	0.69kV
AC Grid Voltage	132kV
Nominal Frequency	50Hz
Transformer rated Power	840MVA
Transformer Voltage ratio	132/0.69kV
Transformer Reactance	0.16pu
Local Load	100MW

Table 3: System parameters (MMC)

Item	MMC ₁	MMC ₂	MMC ₃
Arm inductance	13%	13%	13%
Number of cells per arm (N)	350	350	350
Cell Capacitance	7.2mF	10.8mF	5.4mF
Average Cell capacitance	20.55μF	30.83μF	15.4μF

4 Simulations Assessments of the DC Grid

This section assesses the performance of the DC grid in Fig. 4 when it is operating under the following control modes and operating conditions summarised in Table 4, including the operating mode of each converter terminal and instances of inceptions of three-phase symmetrical AC faults in the AC sides of carefully selected converter terminals.

Table 4: Summary of the operating conditions of the converter terminals and instances of the applications of symmetrical three-phase AC faults in the AC sides of individual converters

Station	Conventional method	Fault	Droop method 1	Fault	Droop method 2	Fault
MMC₁	P and Q	At 8s	Droop and Q	At 8s	Droop and Q	At 8s
	P= 400MW V _{ac} =275kV		V _{dc} = 646 kV V _{ac} =275kV		P= 600MW V _{ac} =275kV	
MMC₂	V _{dc} and Q	At 12s	V _{dc} and Q	At 12s	V _{dc} and Q	At 12s
	V _{dc} = 640kV Q=300MVAr		V _{dc} = 640kV Q=300MVAr		V _{dc} = 640kV Q=300MVAr	
MMC₃	V _d and V _q	At 10s	V _d and V _q	At 10s	V _d and V _q	At 10s
	Islanded Mode		Islanded Mode		Islanded Mode	

4.1 Conventional control method

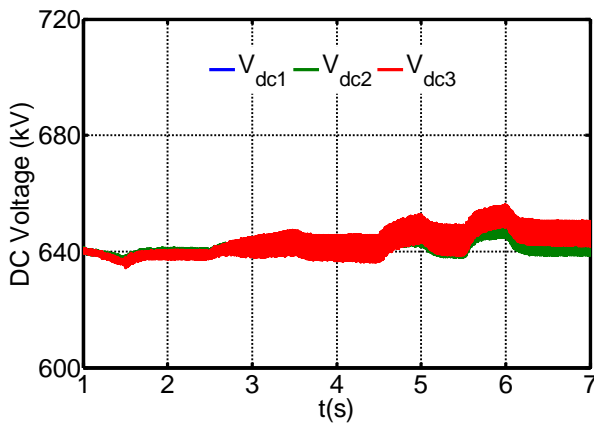
4.1.1 Normal Steady-State Operation

This section assesses the performance of conventional control method applied in DC grid when its control terminals vary their active and reactive power exchange with their respective AC grids and wind farm. Fig. 6 shows simulation waveforms when the DC grid operates under the conventional control method, with the set-points of the stations MMC₁, MMC₂ and MMC₃ as follows:

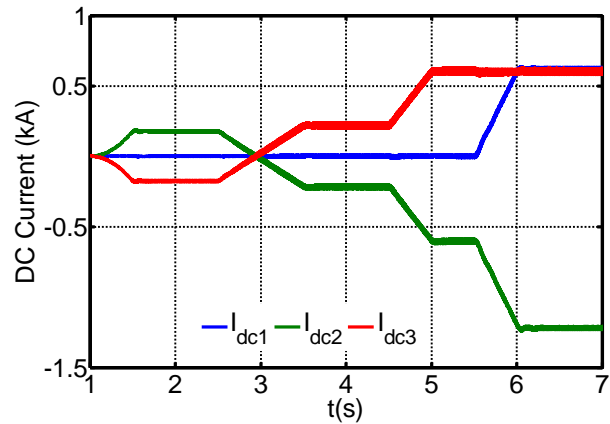
- Initially, MMC₁ controls active power at 0, and at t=5.5s, it varies active power from 0 to 400MW at a rate of 800MW/s and also MMC₁ constantly controls its local AC voltage at 275kV (line-to-line).
- MMC₂ controls DC voltage at 640kV (pole-to-pole), and at t=2.5s, it ramps up its reactive power output from 0MVar to 300MVar at a rate of 600MVar/s.
- At the start, the local AC network connected to MMC₃ is de-energised, and at t=1.5s, it starts building up AC voltage from 0 to rated value of 132kV within 0.5s.
- Wind farm (WF) connected to MMC₃, start ramps its active power from zero to 250MW at 2.5s at a rate of 500 MW/s and finally at 4.5s ramps its power up to 500MW at a rate of 1000MW/s. At t=2.5s, it also ramps up its reactive power output from 0MVar to 100MVar at a rate of 200MVar/s.

Fig. 6 (a), (b), (c) and (d) show the pole-to-pole DC voltages, DC currents, and active and reactive powers of the three converter stations (MMC₁, MMC₂ and MMC₃) and the wind farm (WF) when DC grid is operated under conventional control method and subjected to operation conditions summarised above. Positive directions of active power are assumed to be from AC grids toward converters. It worth recalling that the differences between P₃ and P_{WF} are due to local load consumption of 100MW, with both wind farm and MMC₃ follow the same convention stated above for definition of power flow direction. Fig. 6 (f), and (g) display the R.M.S values of the line-to-line AC voltages and the AC line currents measured at the grid side whereas the converters side AC current is shown in Fig. 6(h).

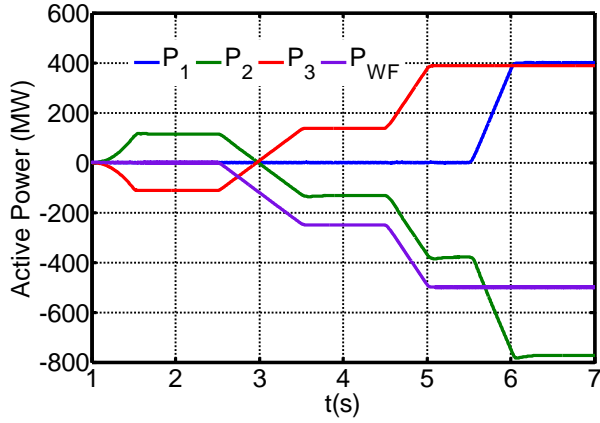
From the waveforms shown in Fig. 6, the main observations are summarised as follows.



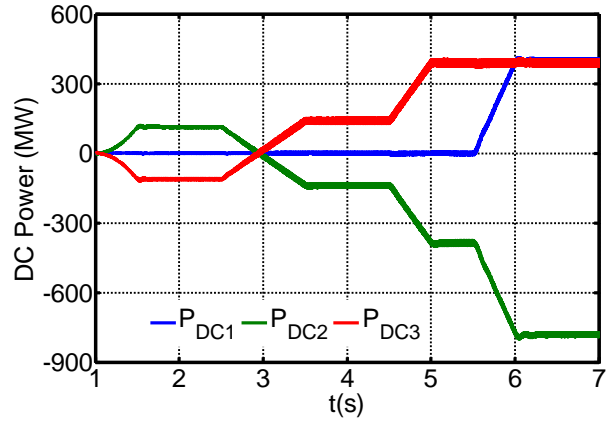
(a) DC voltage



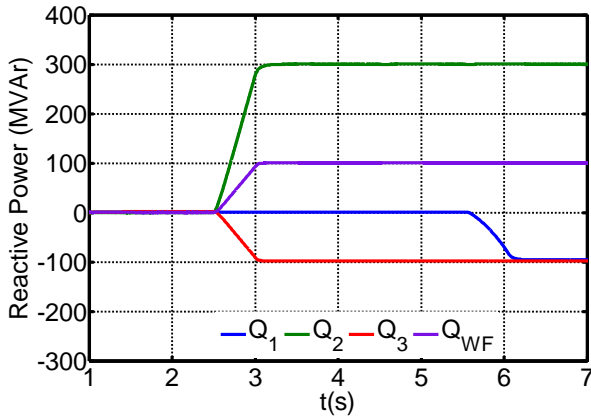
(b) DC current



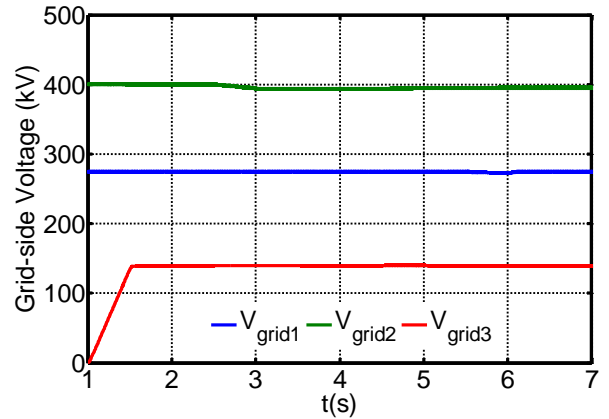
(c) Active Power



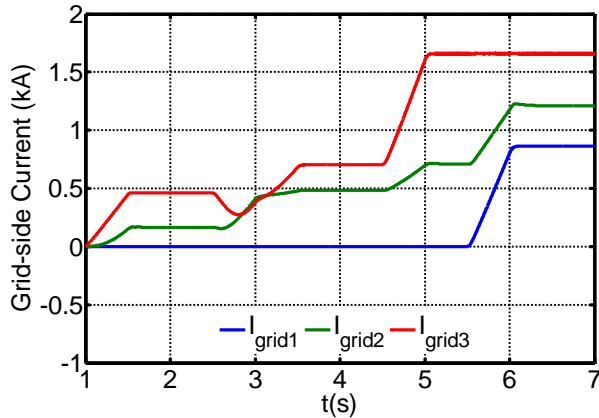
(d) DC Power



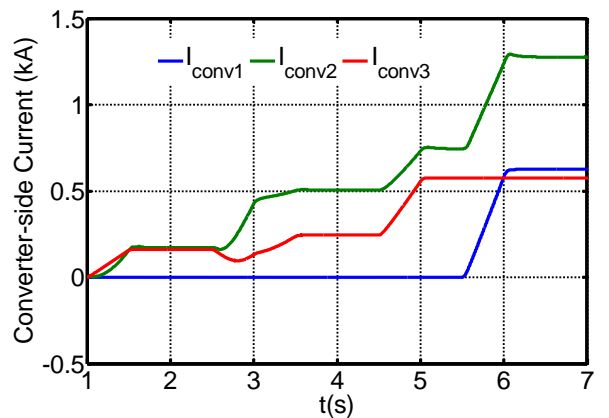
(e) Reactive Power



(f) Grid-side Voltage



(g) Grid-side Current



(h) Converter-side Current

Fig. 6: Simulation waveforms that illustrate the performance of a DC grid during normal operation.

When the DC grid is operated with conventional control method where one of the MMC converter terminals is strictly regulated the DC voltage (PI) at a specified value, the DC voltages of the remaining

MMCs that regulate active powers vary within a narrow range around the set-point by the DC voltage regulator (PI). This entails that the voltage stresses on the MMC switching devices and cell capacitors vary within a tight range around the nominal values. The simulation waveforms in Fig. 6 show that the converter terminals remain capable of controlling reactive powers and AC voltages, independent of active power exports and imports.

With the conventional control method, the converter terminal that regulates DC voltage, i.e. MMC₂, behaves as a slack bus, i.e. balancing the active and DC powers in the DC grid. Therefore, the converter terminal to be designated as DC voltage controller (PI) is ideally to be located in the strongest AC grid that can sink or source active power without creating a significant drift of the power frequency from the nominal. As converter station MMC₂ directly controls its reactive power exchange with the AC grid, its terminal voltage varies noticeably during the change of its reactive power output, see Fig. 6 (e) and (f).

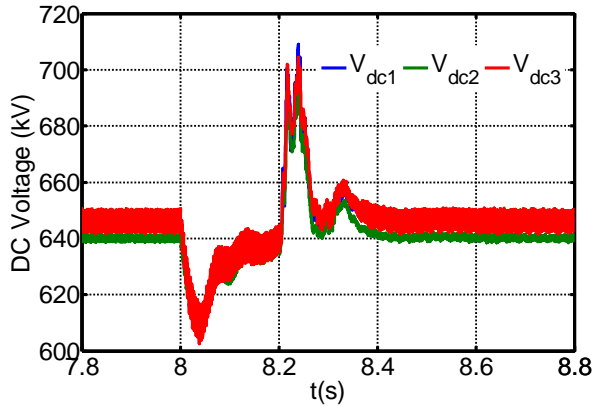
4.1.2 Symmetrical Three-phase AC Fault in the AC side of station MMC₁

This section examines the AC fault ride-through performance of conventional control method when the system is subjected to a symmetrical three-phase AC fault in the AC side of the active power controlling converters MMC₁. Fig. 7 shows simulation waveforms when the DC grid operates under the conventional control method, with the set-points of the stations MMC₁, MMC₂ and MMC₃ as follows:

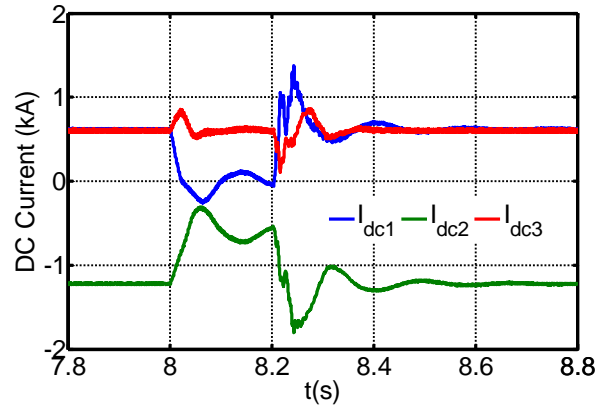
- In the pre-fault condition, MMC₁ controls its active power at 400MW and MMC₁ constantly controls its local AC voltage at 275kV (line-to-line). The same set-points are maintained throughout the simulation for illustration purposes.
- MMC₂ controls DC voltage at 640kV (pole-to-pole) and maintains its reactive power exchange with the AC grid at 300MVar throughout the simulation periods (pre-fault, fault and post-fault periods).
- Throughout the simulation periods (pre-fault, fault and post-fault periods), MMC₃ maintains its local AC voltage at 132kV (line-to-line), and the wind farm generates a constant 500MW power.
- At t=8s, a temporary solid symmetrical three-phase fault is applied in the AC side of MMC₁ with 200ms fault duration.

The main observations drawn from simulations waveforms displayed in Fig. 7 are summarised as follows.

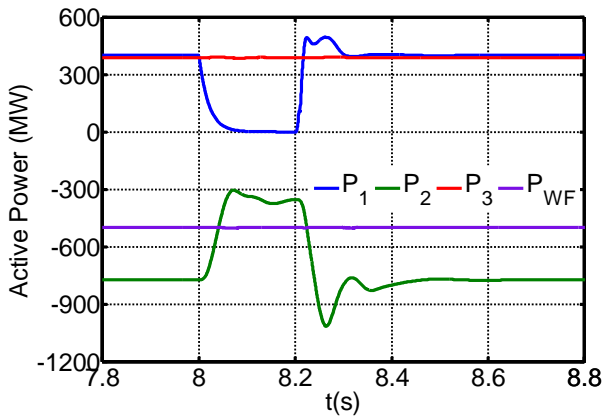
Fig. 7 (a) shows the DC voltages of all converter terminals of the DC grid drop at the instant of the inception of a solid three-phase symmetrical AC fault in the AC terminals of station MMC₁, see AC voltage of station MMC₁ in Fig. 7 (f). Fig. 7 (c) and (e) show the immediate drop of the active and reactive powers of station MMC₁ to zeros as a result of the solid three-phase AC fault. Observe that although the active power of MMC₁ drops to zero during the AC fault period, the DC link current and DC power monitored at the DC terminals of station MMC₁ do not fall to zero, see Fig. 7 (b) and (c); thus, creating a significant imbalance between active power and DC power of the MMC₁, see Fig. 7 (c) and (d). The difference between the active and DC powers of MMC₁ is provided or absorbed by the MMC cell capacitors (in this case, the power imbalance has led to drop of the cell voltages as significant DC power has been extracted from the MMC cell capacitors, though the waveforms are not shown here).



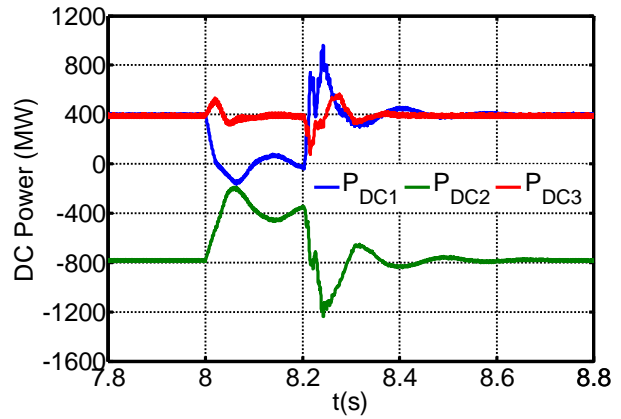
(a) DC voltage



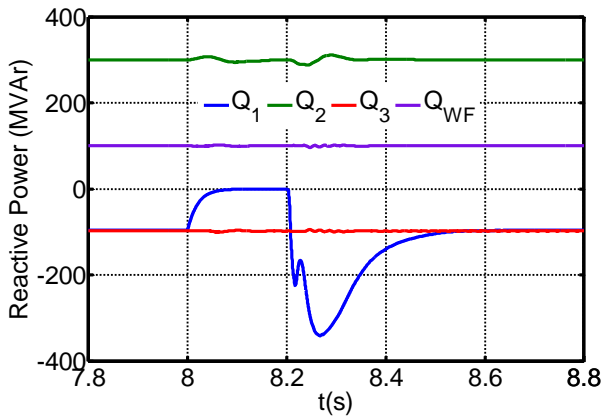
(b) DC current



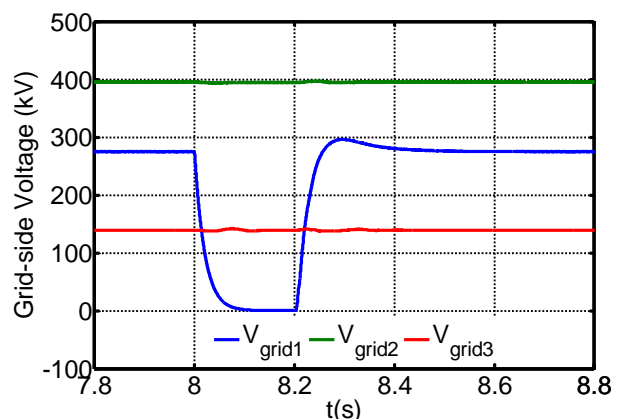
(c) Active Power



(d) DC Power



(e) Reactive Power



(f) Grid-side Voltage

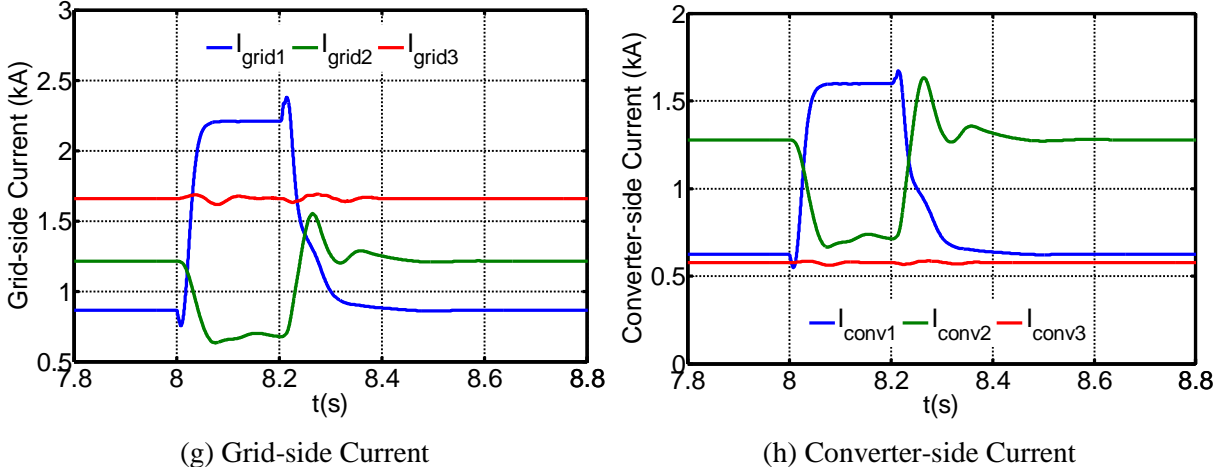


Fig. 7: Simulation waveforms that illustrate the AC fault ride-through performance of DC grid when considering conventional control method and subjected to solid three-phase AC fault in the AC side of the station MMC₁.

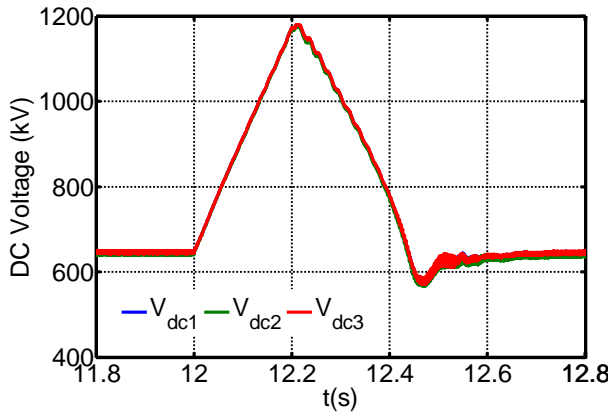
The rapid recovery in the DC voltages of the converter terminals following initial drop at the instant of fault inception is initiated autonomously by the DC voltage controlling converter MMC₂ that acts as power balancer (slack bus). This means in the process of restoring the DC voltage to the specified set-point, MMC₂ must adjust its active power exchange with its AC grid to eliminate the power imbalance created as a result of the AC fault. When the AC fault is cleared at 8.2s, the AC power of station MMC₁ quickly recovers as shown in Fig. 7 (c). The results in DC over-voltages as observed in Fig. 7 (a) due to the sudden increase in the amount of DC power in the DC grid while station MMC₂ requires a finite time to adjust its active power in order to control the DC voltage. The plots in Fig. 7 (e) and (f) confirm that the AC grids connected through DC grid retain their independents, with the impacts of AC fault in one AC grid are seen as power mismatch in the healthy AC grids, see Fig. 7 (c), (g) and (h). The increases observed in the magnitudes of the AC currents of MMC₂ that controls DC voltage and shown in Fig. 7 (g) and (h) are due to active power adjustments at MMC₂.

On the basis of the results in Fig. 7, it can be concluded the conventional control method DC grid can ride-through AC faults that occur in the AC sides of the power controlling converters, without significant difficulties.

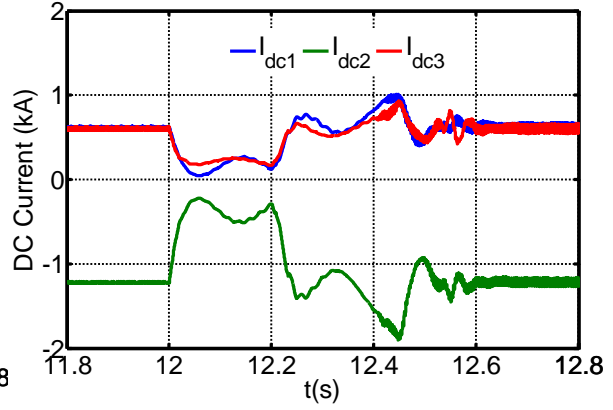
4.1.3 Symmetrical three-phase AC fault in the AC side of station MMC₂

This section examines the performance of the conventional control method when the system is subjected to a solid symmetrical three-phase AC fault in the AC side of the only DC voltage controlling converter MMC₂. Fig. 8 shows simulation waveforms when the DC grid operates under the conventional control method, with the same active and reactive set-points for MMC₁, MMC₂ and MMC₃. The fault is applied at $t=12s$ in the AC side of station MMC₂ that controls DC voltage, with 200ms fault duration.

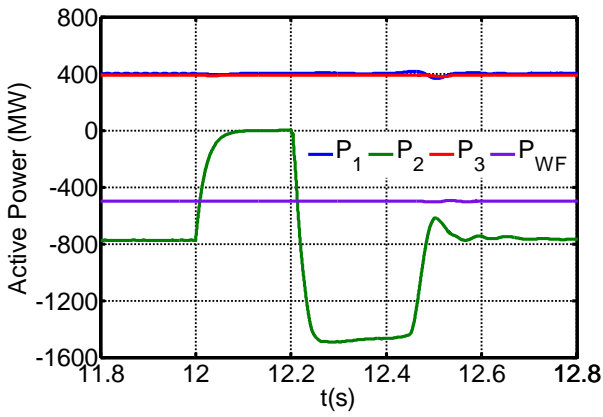
The main observations drawn from simulations waveforms displayed in Fig. 8 are summarised as follows.



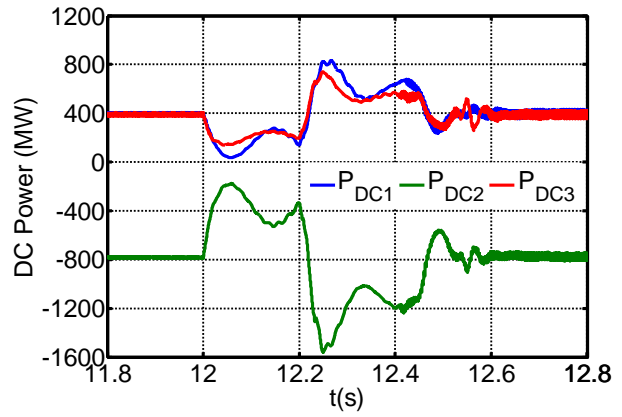
(a) DC voltage



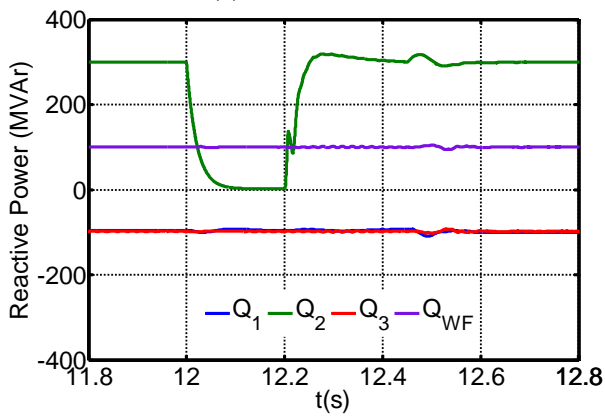
(b) DC current



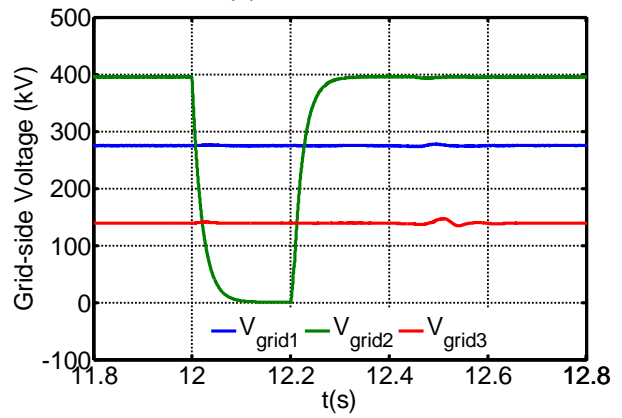
(c) Active Power



(d) DC Power



(e) Reactive Power



(f) Grid-side Voltage

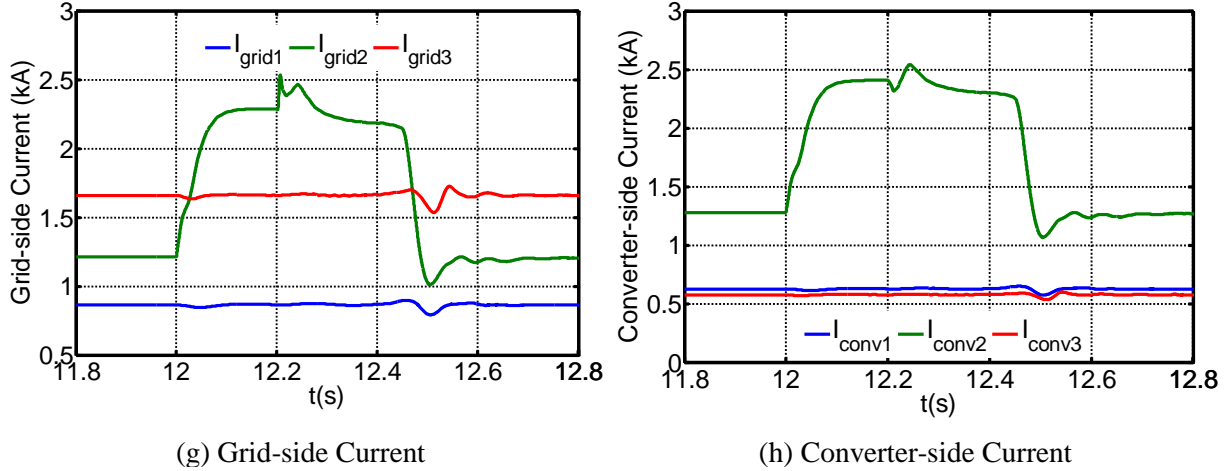


Fig. 8: Simulation waveforms that illustrate the performance of a DC grid when controlled by a conventional control method and subjected to an AC fault in the DC voltage controlling converter station (MMC₂).

Fig. 8 (a) shows an excessive rise of the DC voltages of all converter terminals across the DC grid. The rise of the DC voltages starts at the instant of fault inception in the AC terminals of station MMC₂ and the DC voltages start to decay at instant of fault clearance, see AC voltage of station MMC₂ in Fig. 8 (f). This means during the entire period, the control over the DC voltage is lost, so the DC voltage throughout the DC grid will be driven by the net power imbalance between AC and DC powers. Fig. 8 (c) and (e) show the active and reactive powers of the station MMC₂ that suffers AC fault drop to zeros, but the DC link current and DC power monitored at the DC terminals of station MMC₂ do not fall to zero, see Fig. 8 (b), (c), (e) and (f). On the other hand, the converter stations MMC₁ and MMC₃ maintain their pre-fault active power set-points, exacerbating the power imbalance between the AC and DC sides; thus, worsening the rise of DC voltage across the DC grid, Fig. 8 (c) and (d).

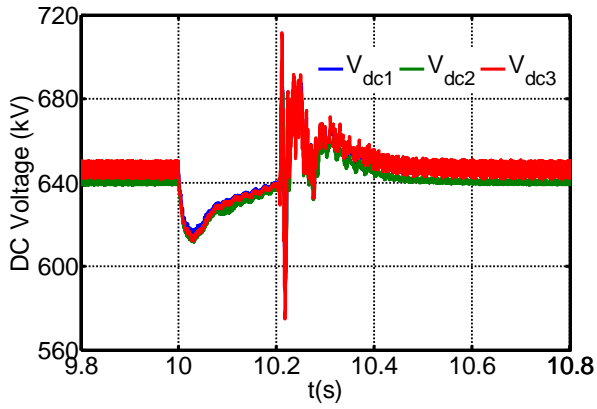
Although the DC grid quickly recovers the control over the DC voltage following AC fault clearance, the risk of total loss of controllability remains high when conventional control method is used, particularly, if the AC fault is sustained over a long period for the worst-case operating condition that corresponds to the largest power imbalance. Unlike the previous case, AC voltages, active and reactive powers, and AC currents in the healthy AC grids remain unaffected, which confirm the decoupling of the AC grids, Fig. 8 (e), (f), (g) and (h).

On the basis of the results in Fig. 8, it can be concluded that the conventional control method with one dedicated DC voltage controlling converter is inappropriate as it does not offer the necessary level of security required for reliable operation of the DC grid. Designation of more than one converter for controlling DC voltage must be implemented.

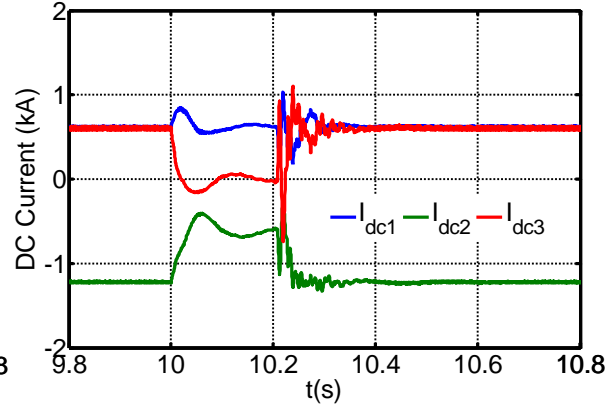
4.1.4 Symmetrical three-phase AC fault in the AC side of station MMC₃:

This section examines the performance of the conventional control method when the system is subjected to a solid symmetrical three-phase AC fault in the AC side of the converter station MMC₃. Fig. 9 shows simulation waveforms when the DC grid operates under the conventional control method, with same set-

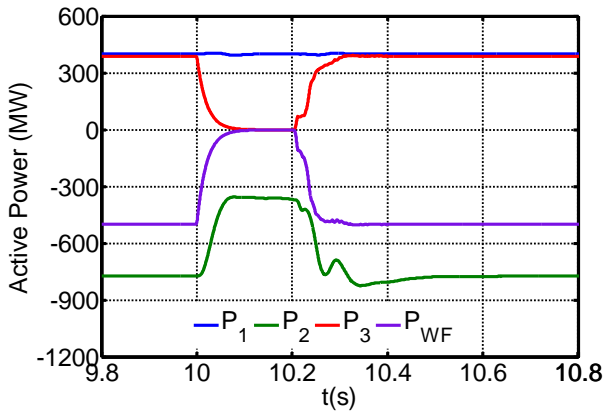
points of MMC₁, MMC₂ and MMC as previous studies. A temporary fault is applied in the AC side of MMC₃ at t=10s with 200ms fault duration. The main observations drawn from simulations waveforms displayed in Fig. 9 are summarised as follows.



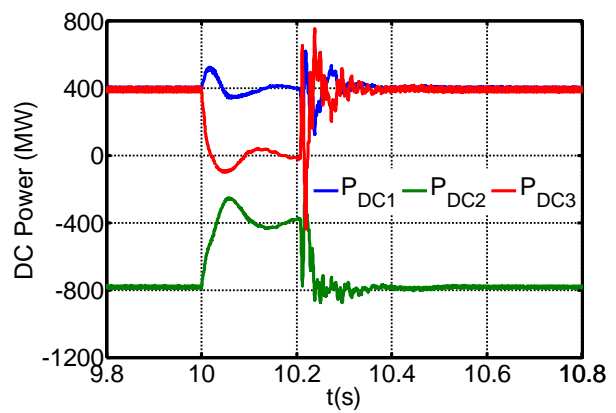
(a) DC voltage



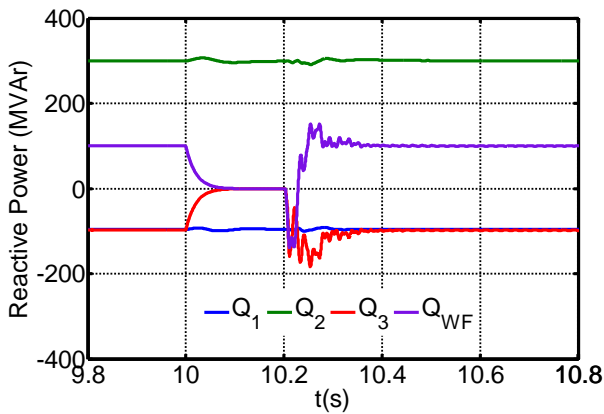
(b) DC current



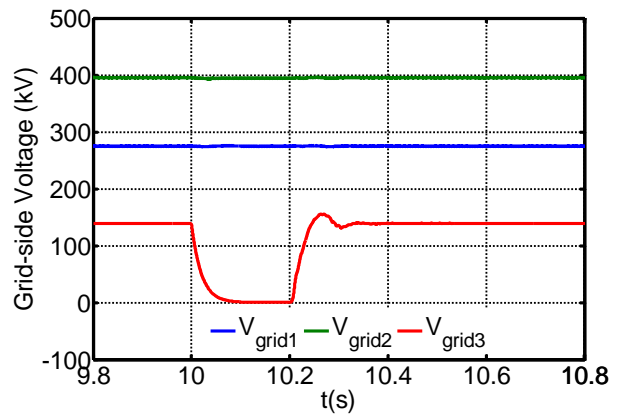
(c) Active Power



(d) DC Power



(e) Reactive Power



(f) Grid-side Voltage

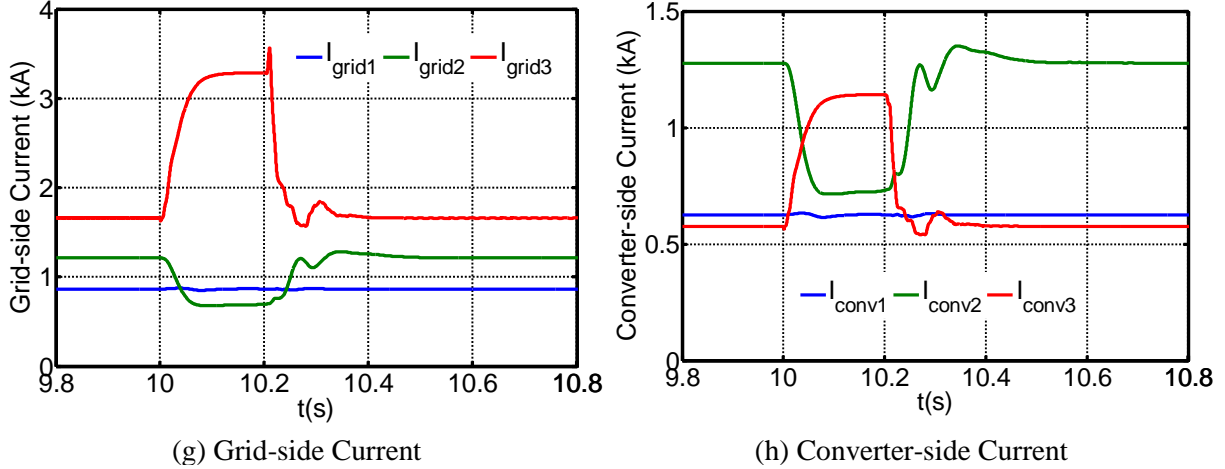


Fig. 9: Simulation waveforms that illustrate the performance of a DC grid when it is controlled by conventional control method and subjected to an AC fault in the AC side of station MMC₃

Fig. 9 (a) shows the DC voltages of all converter terminals drop at the instant of the inception of the AC fault at MMC₃ which reduces the wind farm AC voltage at the MMC₃ terminal to zero as shown in Fig. 9(f). Fig. 9 (c) and (e) show the immediate drop of the active and reactive powers of station MMC₃ to zeros as a result of the solid three-phase AC fault. The active power of MMC₁ is largely unaffected and MMC₂ adjust its active power in order to control the DC voltage back to the set-point of 640kV as can be seen in Fig. 9 (a)-(d).

When the AC fault is cleared at 10.2s, the wind farm AC voltage is quickly restored by MMC₃ and consequently, active powers generated by the wind farm and transmitted to the DC grid by MMC₃ rapidly recover as seen in Fig. 9 (c) and (f). This leads to excessive power on the DC grid as MMC₂ requires a finite time to adjust its active power, and consequently, results in DC over-voltages observed in Fig. 9 (a). The plots in Fig. 9 (e) and (f) confirm that the AC grids connected through the DC grid retain their independents, with the impacts of AC fault in one AC grid are seen as power mismatch in the healthy AC grids, see Fig. 9 (c), (g) and (h). The increases observed in the magnitudes of the AC currents of MMC₃ shown in Fig. 9 (g) and (h) are due to active power adjustments.

4.2 Droop Control-Method 1

This section presents a quantitative evaluation of droop method during normal operation with converter terminals vary their active power, reactive power and AC voltage set-points, and worst-case AC fault scenario (solid three-phase AC faults in the AC side of the DC voltage controlling converter MMC₂).

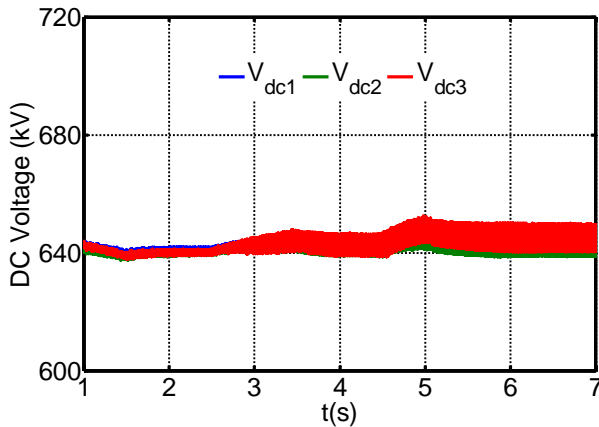
4.2.1 Normal Operation

This subsection assesses the performance of droop method 1 when it is applied to the DC grid. Fig. 10 shows simulation waveforms when the DC grid is operated as follows:

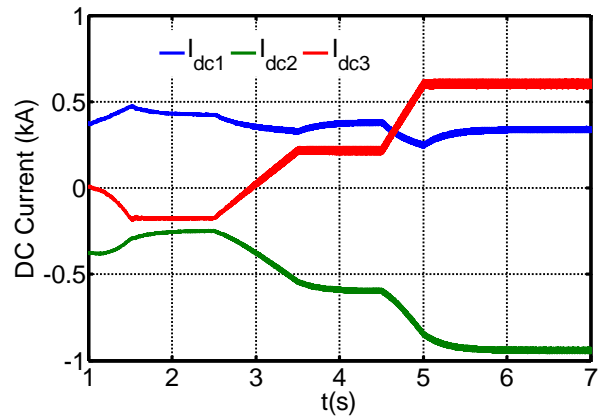
- Station MMC₁ is equipped with droop method 1 so that it can control its DC voltage (droop) with predefined set-point and also MMC₁ constantly controls its local AC voltage at 275kV (line-to-line).
- MMC₂ operating conditions as follows:

- From start, station MMC₂ controls DC voltage (PI) at 640kV (pole-to-pole).
- At t=2.5s, it ramps up its reactive power output from 0 to 300MVAR at a rate of 600MVAR/s.
- MMC₃ builds up its local wind farm AC voltage from 1s-1.5s. The local load is 100MW. At 2.5s the wind farm starts ramps its active power from zero to 250MW at a rate of 500MW/s and at 4.5s, it ramps up to 500MW at a rate of 1000MW/s. At t=2.5s, its reactive power output is increased from 0MVAR to 100MVAR at a rate of 200MVAR/s.

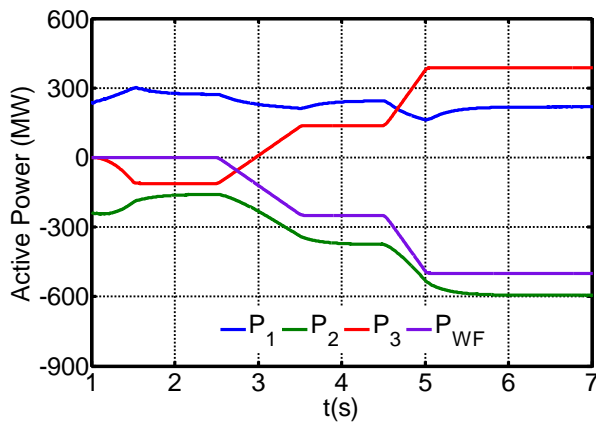
Fig. 10 (a)-(e) show the DC voltages, DC currents, and active powers, DC powers and reactive powers of the three converter stations (MMC₁, MMC₂ and MMC₃). Fig. 10 (f), (g) and (h) display the R.M.S values of the grid side line-to-line AC voltages and of the line currents measured at the grid and converter AC grid sides of the converter stations, respectively. From the simulation waveforms shown in Fig. 10, the main observations are summarised as follows. As shown in Fig. 10 (c), initially MMC₃ imports from DC to the local AC to supply the 100MW local load. Once the wind power generation becomes more than the local load demand, MMC₃ automatically reverse power flow direction and exports power from wind farm network to the DC grid.



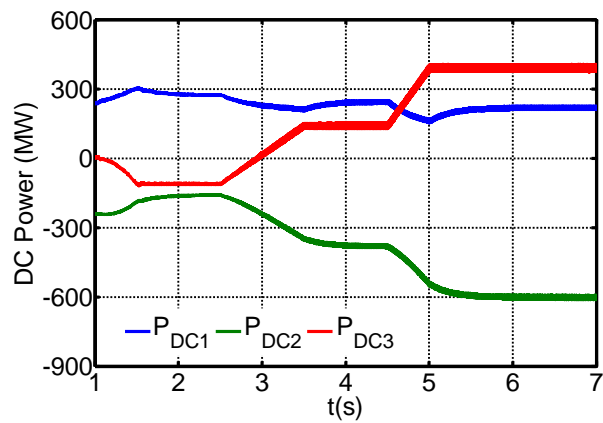
(a) DC voltage



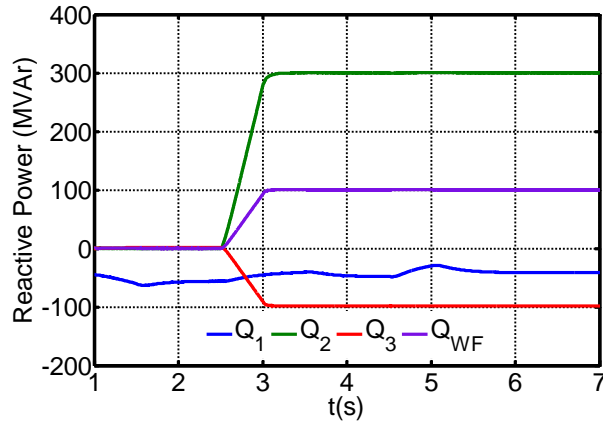
(b) DC current



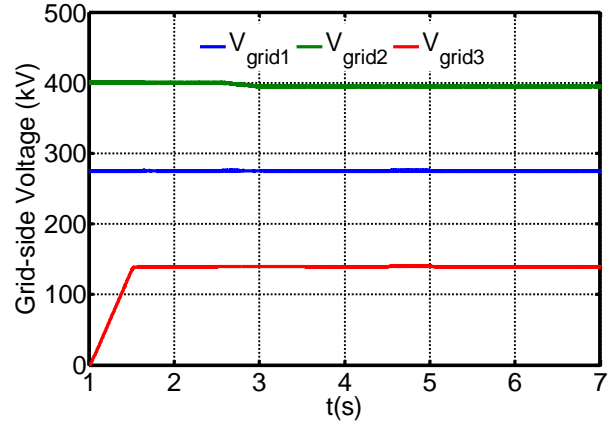
(c) Active Power



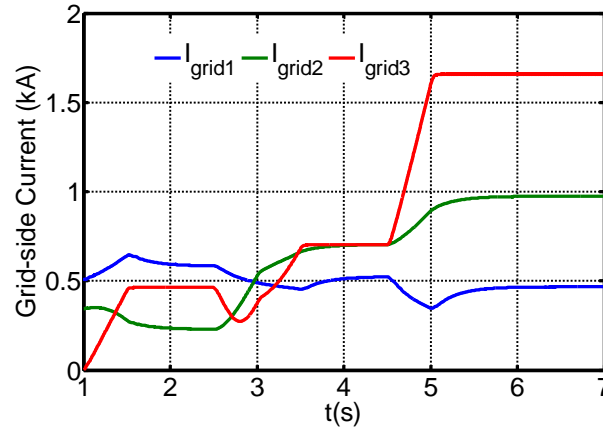
(d) DC Power



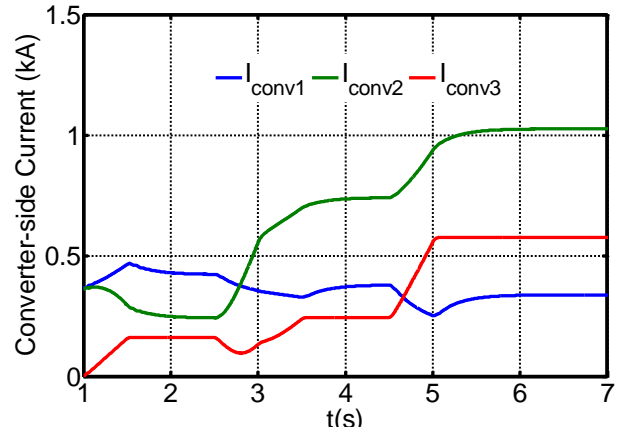
(e) Reactive Power



(f) Grid-side Voltage



(g) Grid-side Current



(h) Converter-side Current

Fig. 10: Simulation waveforms that illustrate the performance of a DC grid during normal operation using droop method in station MMC₁

When the DC grid is operated with droop method 1 at MMC₁ and constant DC voltage control at MMC₂, the DC voltages across the DC grid vary within a range around that sets by the DC voltage controlling converter. This is desirable as the voltage stresses on the MMC switching devices and cell capacitors remain tightly controlled within a small range around the nominal values. The simulation waveforms in Fig. 10 show that all converter stations are capable of exchanging power among them with the AC grid.

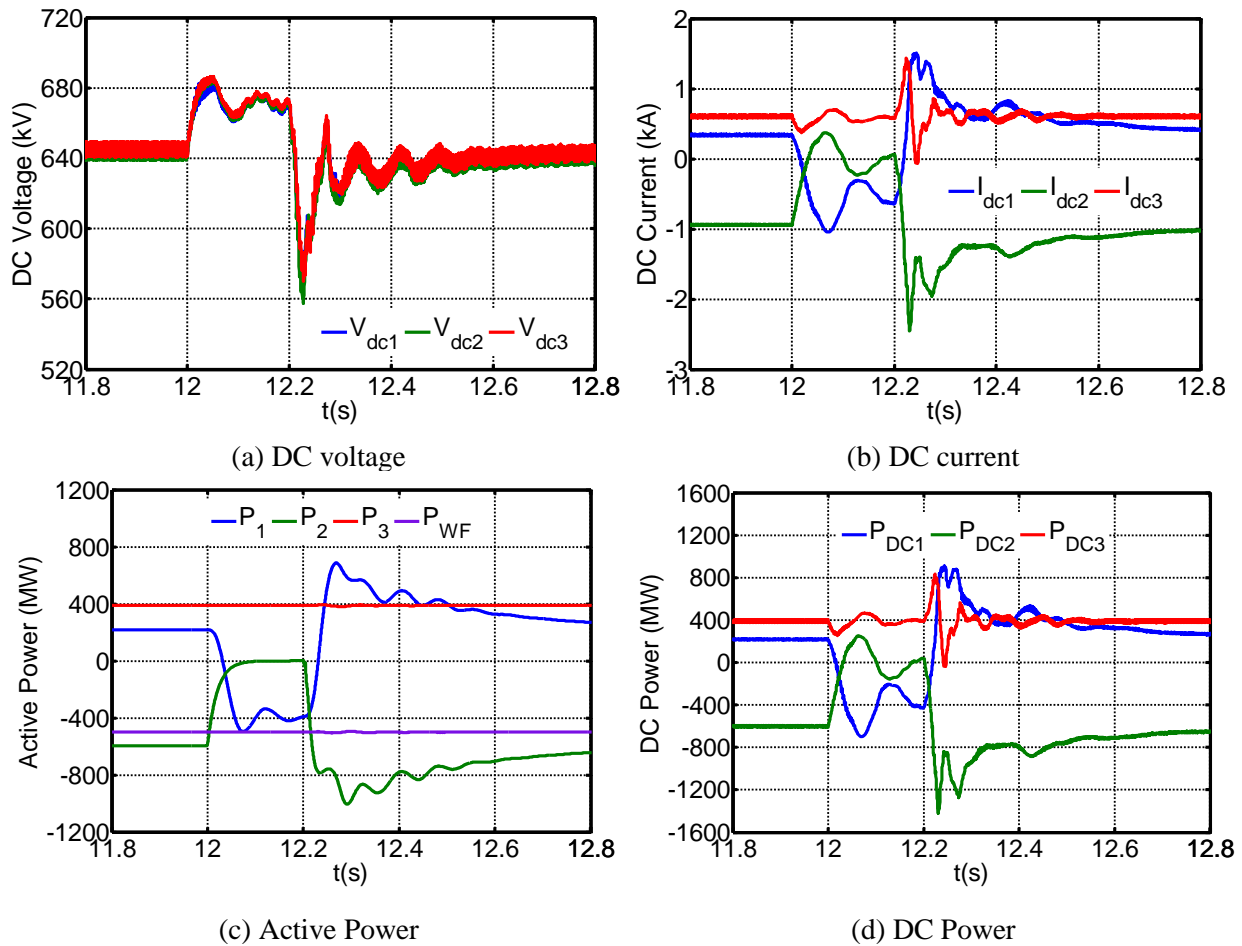
4.2.2 Symmetrical Three-phase AC fault at MMC₂

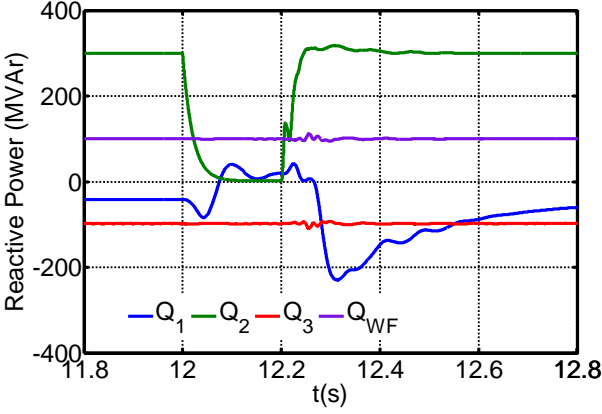
This section examines an AC fault ride-through performance of the DC grid when droop method 1 is incorporated in MMC₁ and subjected to a solid symmetrical three-phase fault in the AC side of the only DC voltage (PI) controlling converter (MMC₂ in this illustrative case) at $t=12s$ with 200ms fault duration. The main observations are drawn from simulations waveforms displayed in Fig. 11 are summarised as follows.

Fig. 11 (a) shows a modest rise of the DC voltages of all converter terminals across the DC grid in Fig. 4. Observe that the rise of the DC voltages start at the instant of AC fault inception in the AC terminals of

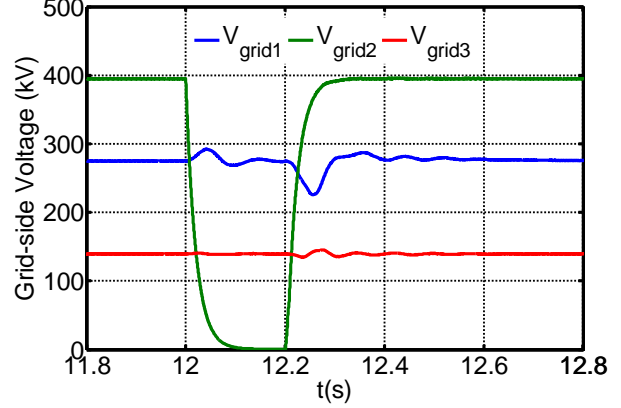
station MMC₂, but the DC voltages are stabilised as MMC₁ that operates with droop method 1 temporarily takes over the function of DC voltage regulation. Fig. 11 (c) and (e) show the active and reactive powers of the station MMC₂ that suffers AC fault drop to zeros, though the DC link current and DC power monitored at the DC terminals of station MMC₂ do not fall to zero as previously explained, see Fig. 11 (b), (c), (e) and (f). On the other hand, MMC₁ quickly controls its DC voltage at its predefined set-point, while station MMC₃ retains its pre-fault active power setting. Thus, loss of DC voltage controlling converter MMC₂ does not mean total loss of control over the DC voltage of the DC grid, see Fig. 11 (c) and (d). This illustrative example shows the droop method 1 implemented in MMC₁ helps to maintain power balance during AC fault. The plots for the AC voltages, active and reactive powers, and AC currents in the healthy AC grids remain unaffected, which means incorporation of the droop method 1, see Fig. 11 (e), (f), (g) and (h). Once the fault is cleared, the whole system gradually recovers with limited oscillations. In this study, the purpose is to show the effect of droop method 1 on DC voltage control and no controller optimisation is attempted.

On the basis of the results shown in Fig. 11, it can be concluded that droop method 1 is conducive normal operation and AC fault ride-through of the AC fault of the DC grid.

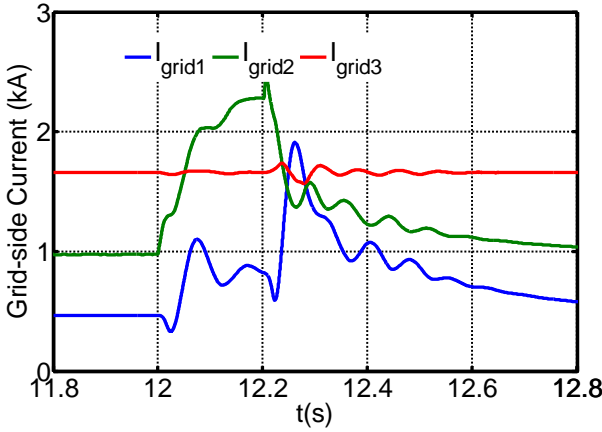




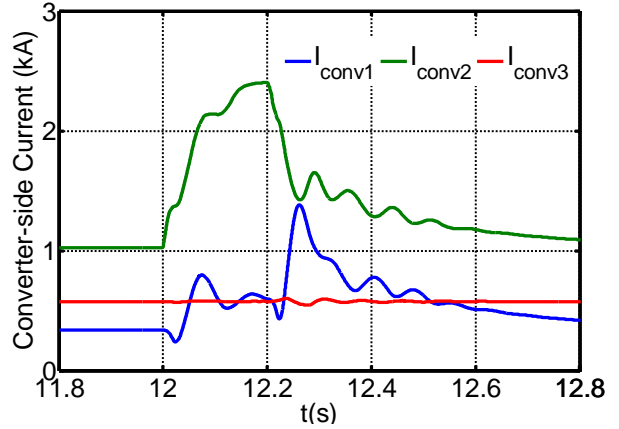
(e) Reactive Power



(f) Grid-side Voltage



(g) Grid-side Current



(h) Converter-side Current

Fig. 11: Simulation waveforms that illustrate the AC fault ride-through performance of DC grid when converter MMC₂ is subjected to an AC fault in its AC side

4.3 Droop Control-Method 2

This section presents a quantitative evaluation of droop method 2 during normal operation with converter terminals vary their active power, reactive power and AC voltage set-points, and worst-case AC fault scenario (solid three-phase AC faults at MMC₂).

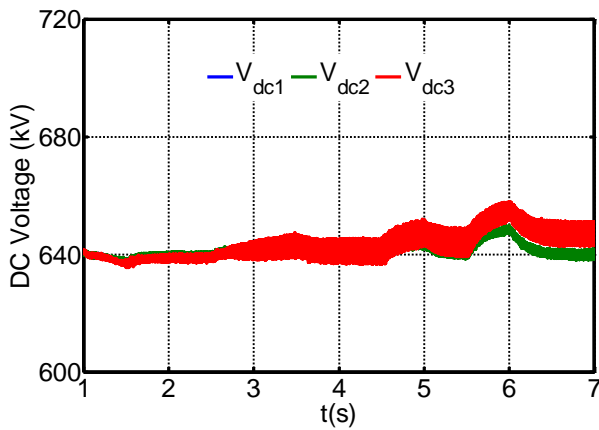
4.3.1 Normal Operation

Fig. 12 shows simulation waveforms when the DC grid is operated as follows:

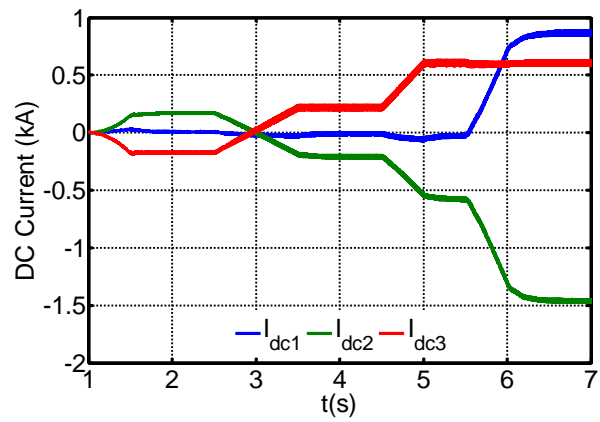
- Station MMC₁ is equipped with droop method 2 and its active power and AC voltage control set-points are:
 - During $0 \leq t < 5.5s$, active power is controlled at 0.
 - At $t=5.5s$, it ramps up active power from 0 to 600MW at a rate of 1200MW/s.
 - MMC₁ constantly controls its local AC voltage at 275kV.
- MMC₂ operating conditions as follows:

- From the start, station MMC₂ controls DC voltage at 640kV.
- At t=2.5s, it ramps up its reactive power output from 0 to 300MVAR at a rate of 600MVAR/s.
- MMC₃ builds up its local wind farm AC voltage from 1s-1.5s. The local load is 100MW. At 2.5s the wind farm starts ramps its active power from zero to 250MW at a rate of 500MW/s and at 4.5s, it ramps up to 500MW at a rate of 1000MW/s. At t=2.5s, its reactive power output is increased from 0MVAR to 100MVAR at a rate of 200MVAR/s.

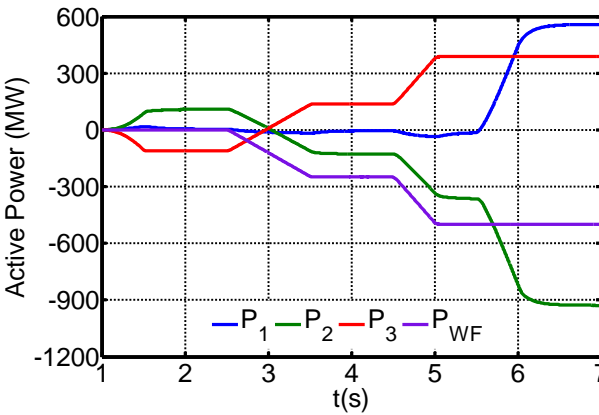
Fig. 12 (a)-(e) show the DC voltages, DC currents, and active powers, DC powers and reactive powers of the three converter stations MMC₁, MMC₂ and MMC₃. Also, in Fig. 12 (c) and (e) show the active and reactive power generated from the wind farm. From the simulations waveforms shown in Fig. 12, the main observations are summarised as follows.



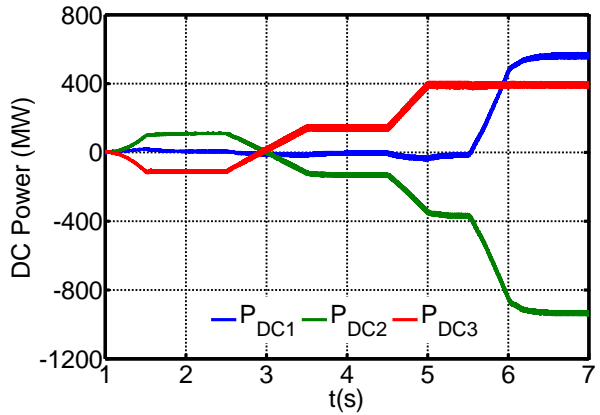
(a) DC voltage



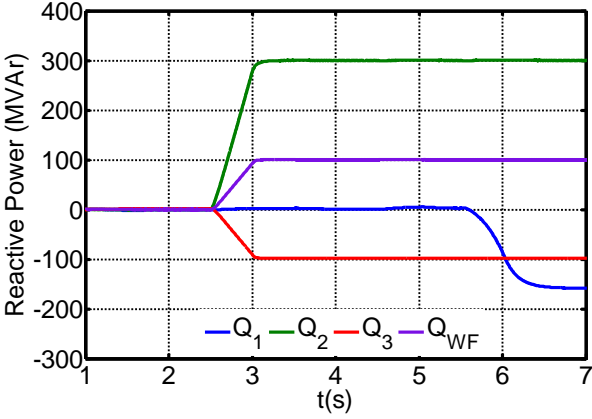
(b) DC current



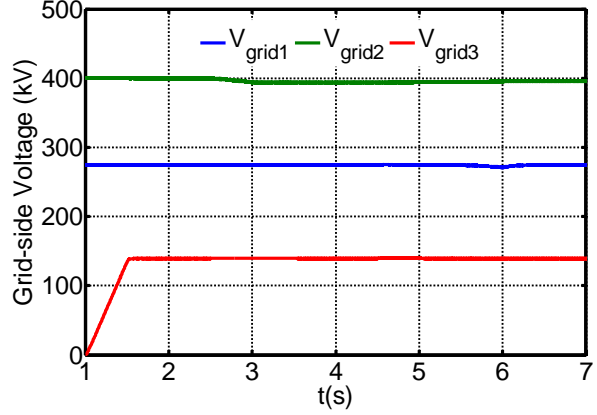
(c) Active Power



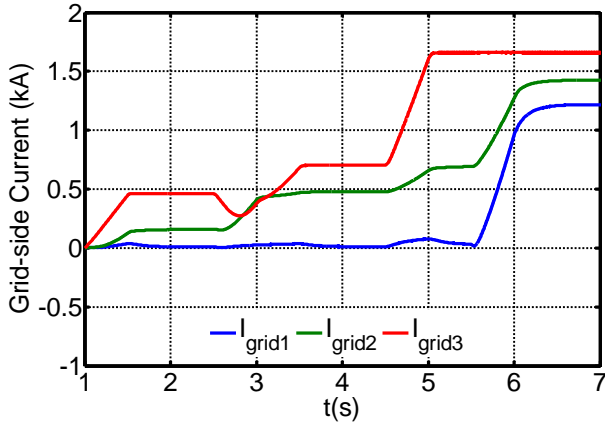
(d) DC Power



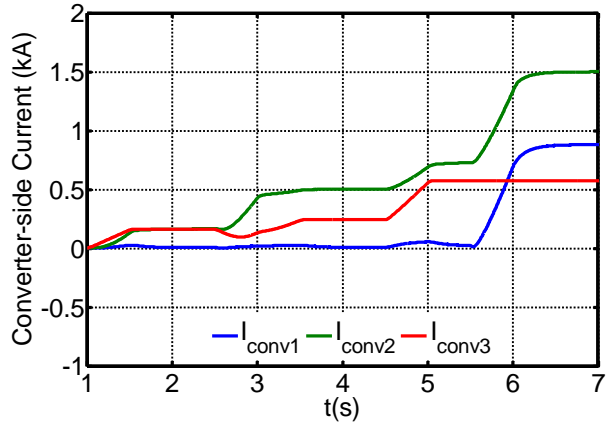
(e) Reactive Power



(f) Grid-side Voltage



(g) Grid-side Current



(h) Converter-side Current

Fig. 12: Simulation waveforms that illustrate the performance of a DC grid during normal operation when droop method 2 is employed in MMC₁

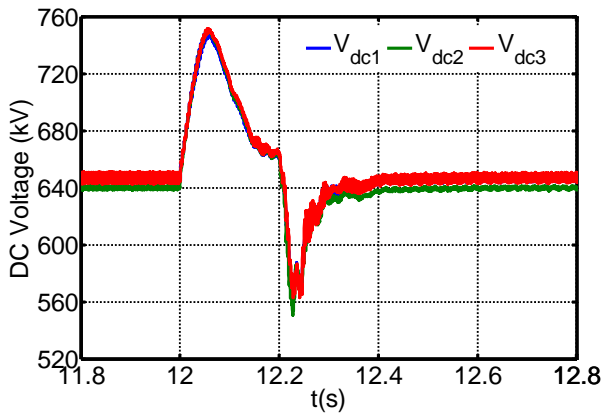
When the DC grid is operated with droop method 2 at MMC₁ with MMC₂ regulating the DC voltage at a specified value of 640kV, the DC voltages across the DC grid vary within a narrow range around that sets by the DC voltage controlling converter. The simulation waveforms in Fig. 12 shows that the converter MMC₁ remains capable of controlling its active power exchange with the AC grid, and the DC grid when one its terminal is controlled using droop method 2 exhibits similar results to that of the conventional control method discussed in subsection 4.1.

4.3.2 Symmetrical Three-phase AC fault- fault at MMC₂

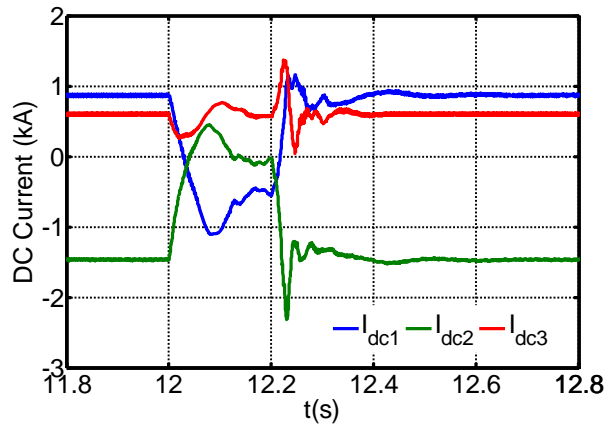
This section examines the performance of the DC grid when droop method 2 is incorporated in MMC₁ and is subjected to a solid symmetrical three-phase AC fault in the AC side of MMC₂. The main observations drawn from simulations waveforms displayed in Fig. 13 are summarised as follows:

Fig. 13 (a) shows a modest rise of the DC voltages of all converter terminals across the DC grid. Observe that the rise of the DC voltages starts at the instant of AC fault inception in the AC terminals of station MMC₂, but the DC voltages stabilise as MMC₁ operates in droop method 2, which temporarily takes over the function of DC voltage regulation. Fig. 13 (c) and (e) show the active and reactive powers of the station MMC₂ that suffers AC fault drop to zeros. On the other hand, MMC₁ quickly adjusts its active power set-point as it switches to DC voltage control while station MMC₃ retains its pre-fault active power setting. Thus, loss of DC voltage controlling converter MMC₂ does not lead to total loss of control over the DC voltage of the DC grid, see Fig. 13 (c) and (d).

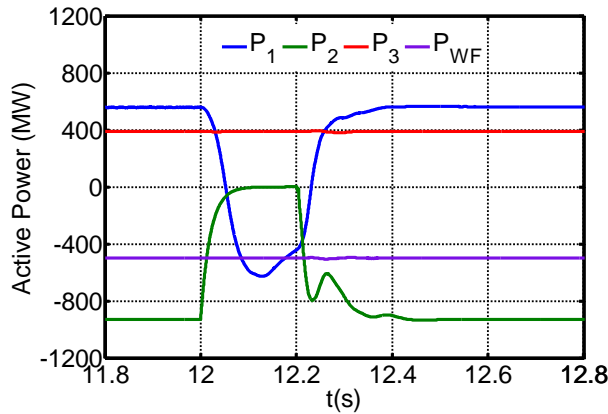
This illustrative example shows droop method 2 implemented in MMC₁ helps to minimize the power imbalance during the AC fault. The terminal with droop method 2 acts as an auxiliary standby DC voltage controlling converter with loosely defined voltage set-point, and helps the DC voltage of the DC grid to recover quickly, following AC fault clearance. In this way, the risk to DC grid stability is minimized. The plots for the AC voltages, active and reactive powers, and AC currents in the healthy AC grids remain unaffected, which means incorporation of the droop method 2 does not compromise decoupling of the AC grids, see Fig. 13 (e), (f), (g) and (h).



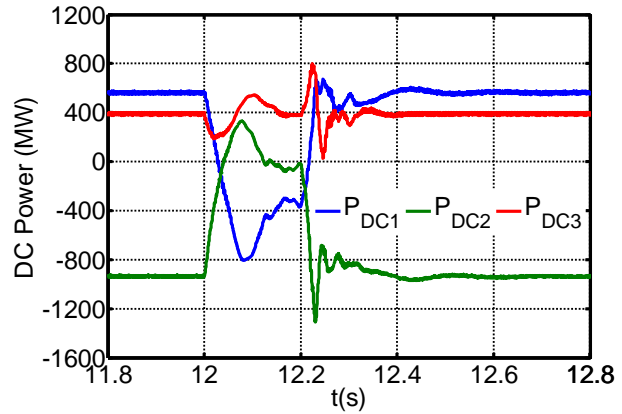
(a) DC voltage



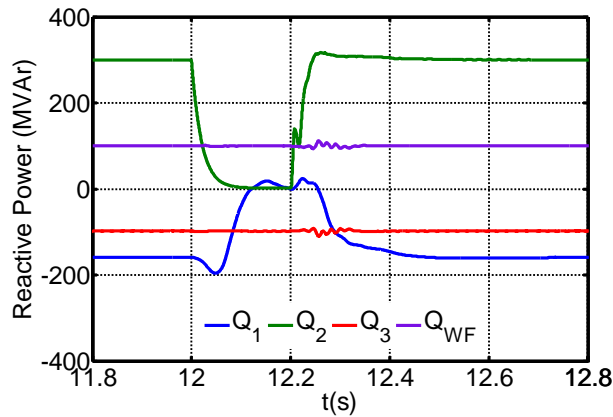
(b) DC current



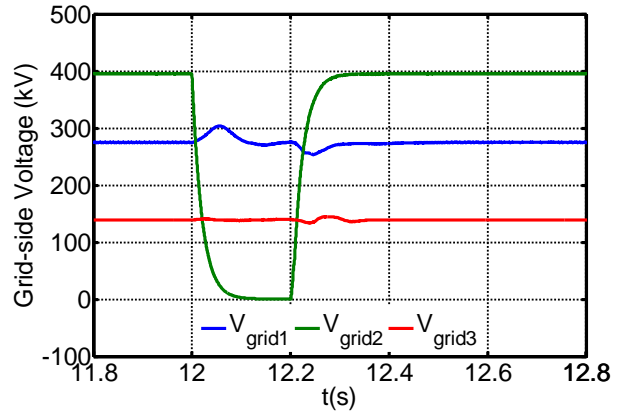
(c) Active Power



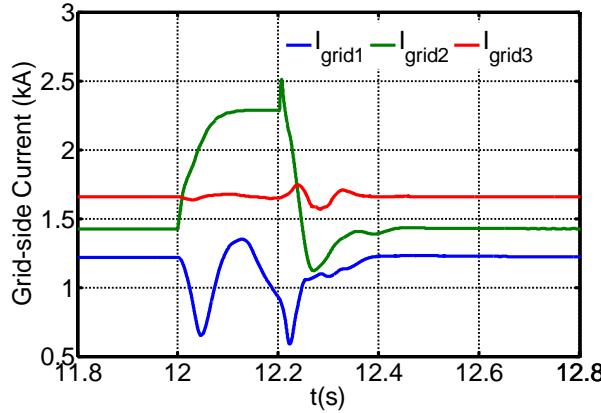
(d) DC Power



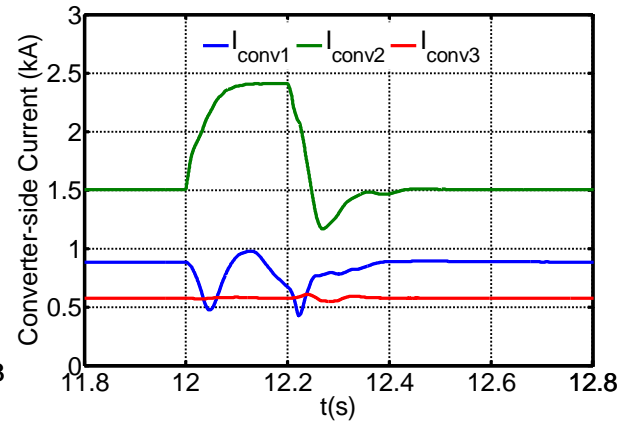
(e) Reactive Power



(f) Grid-side Voltage



(g) Grid-side Current



(h) Converter-side Current

Fig. 13: Simulation waveforms that illustrate the performance of the DC grid when MMC₁ is controlled based on droop method 2 and the other DC voltage controlling converter MMC₂ is subjected to AC fault in its AC side.

5 Conclusions

This report has presented an analysis of a three-terminal DC grid based on averaged HB MMC converter model, with emphasis on the different control modes that offers different operating condition for the system operator. A number of case studies, including normal steady-state operation and AC faults, has been conducted to underpin the various control approach and its advantages. Based on detailed studies conducted in this report, the following conclusions are drawn:

- DC grid operated with conventional control method where one of the converter terminals strictly regulates the DC voltage at a specified value, with the remaining converters regulating active powers, potentially risks total loss of controllability due to severe DC over- or under-voltage during faults on the AC side of the only DC voltage controlling station.

- Droop method 1 is employed in MMC₁ of the converters based on DC voltage droop characteristic to provide adequate DC voltage regulation and power sharing among the connected AC grids. In case of any fault event in the AC side of one of the DC voltage controlling terminals, the other terminal will maintain DC link voltage with limited DC voltage variation. Therefore, droop method 1 will minimize the risk of total loss of controllability, particularly, if the AC fault is sustained over a long period for the worst-case operating condition.
- Droop method 2 implemented in MMC₁ acts as an auxiliary standby DC voltage controlling converter with loosely defined voltage set-point, and helps the DC voltage of the DC grid to recover quickly, following AC fault clearance. In this way, the risk to DC grid stability is also minimized.

The developed DC grid model provides good flexibility for further investigation into DC grid operations with different DC voltage control and power dispatch strategies, the interaction of AC and DC grids including voltage and/or frequency stability, system protection, integration of renewables etc.

6 References

- [1] G. Tang, Z. He, H. Pang, X. Huang, and X. p. Zhang, "Basic topology and key devices of the five-terminal DC grid," *CSEE Journal of Power and Energy Systems*, vol. 1, no. 2, pp. 22-35, 2015.
- [2] H. Rao, "Architecture of Nan'ao multi-terminal VSC-HVDC system and its multi-functional control," *CSEE Journal of Power and Energy Systems*, vol. 1, no. 1, pp. 9-18, 2015.
- [3] L. L. Wang Hao, and Wu Dianfeng. (2014, 27/02/2015). 'Hierarchical control in a 5-terminal VSC-HVDC project'. Available: <http://www.ee.co.za/article/hierarchical-control-5-terminal-vsc-hvdc-project.html>
- [4] L. Tang, "Control and Application of Multi-terminal HVDC based on voltage-Source Converter," Doctor of Philosophy, Electrical and Computer Engineering, McGill University, Montréal, Québec, Canada, 2003.
- [5] K. Rouzbehi, A. Miranian, A. Luna, and P. Rodriguez, "DC Voltage Control and Power Sharing in Multiterminal DC Grids Based on Optimal DC Power Flow and Voltage-Droop Strategy," *IEEE Journal of Emerging and Selected Topics in Power Electronics*, vol. 2, no. 4, pp. 1171-1180, 2014.
- [6] L. Xu, L. Yao, M. Bazargan, and Y. Wang, "The Role of Multiterminal HVDC for Wind Power Transmission and AC Network Support," in *Power and Energy Engineering Conference (APPEEC), 2010 Asia-Pacific*, 2010, pp. 1-4.
- [7] J. Beerten, O. Gomis-Bellmunt, X. Guillaud, J. Rimez, A. v. d. Meer, and D. V. Hertem, "Modeling and control of HVDC grids: A key challenge for the future power system," in *2014 Power Systems Computation Conference*, 2014, pp. 1-21.
- [8] E. Prieto-Araujo, A. Egea-Alvarez, S. Fekriasl, and O. Gomis-Bellmunt, "DC Voltage Droop Control Design for Multiterminal HVDC Systems Considering AC and DC Grid Dynamics," *IEEE Transactions on Power Delivery*, vol. 31, no. 2, pp. 575-585, 2016.
- [9] L. Xu and L. Yao, "DC voltage control and power dispatch of a multi-terminal HVDC system for integrating large offshore wind farms," *Renewable Power Generation, IET*, vol. 5, no. 3, pp. 223-233, 2011.
- [10] J. Beerten, S. Cole, and R. Belmans, "Modeling of Multi-Terminal VSC HVDC Systems With Distributed DC Voltage Control," *IEEE Transactions on Power Systems*, vol. 29, no. 1, pp. 34-42, 2014.
- [11] A. Kirakosyan, E. F. El-Saadany, M. S. E. Moursi, S. Acharya, and K. A. Hosani, "Control Approach for the Multi-Terminal HVDC System for the Accurate Power Sharing," *IEEE Transactions on Power Systems*, vol. 33, no. 4, pp. 4323-4334, 2018.
- [12] C. D. Barker and R. S. Whitehouse, "Further developments in autonomous converter control in a multi-terminal HVDC system," in *10th IET International Conference on AC and DC Power Transmission (ACDC 2012)*, 2012, pp. 1-6.
- [13] T. Nakajima and S. Irokawa, "A control system for HVDC transmission by voltage sourced converters," in *1999 IEEE Power Engineering Society Summer Meeting. Conference Proceedings (Cat. No.99CH36364)*, 1999, vol. 2, pp. 1113-1119 vol.2.
- [14] M. Han, D. Xu, and L. Wan, "Hierarchical optimal power flow control for loss minimization in hybrid multi-terminal HVDC transmission system," *CSEE Journal of Power and Energy Systems*, vol. 2, no. 1, pp. 40-46, 2016.

- [15] J. Cao, W. Du, H. F. Wang, and S. Q. Bu, "Minimization of Transmission Loss in Meshed AC/DC Grids With VSC-MTDC Networks," *IEEE Transactions on Power Systems*, vol. 28, no. 3, pp. 3047-3055, 2013.
- [16] G. Li, Z. Du, C. Shen, Z. Yuan, and G. Wu, "Coordinated Design of Droop Control in MTDC Grid Based on Model Predictive Control," *IEEE Transactions on Power Systems*, vol. PP, no. 99, pp. 1-1, 2017.
- [17] K. Rouzbehi, A. Miranian, J. I. Candela, A. Luna, and P. Rodriguez, "A Generalized Voltage Droop Strategy for Control of Multiterminal DC Grids," *IEEE Transactions on Industry Applications*, vol. 51, no. 1, pp. 607-618, 2015.
- [18] W. Wang, M. Barnes, and O. Marjanovic, "Stability limitation and analytical evaluation of voltage droop controllers for VSC MTDC," *CSEE Journal of Power and Energy Systems*, vol. 4, no. 2, pp. 238-249, 2018.
- [19] L. Xu, L. Yao, and M. Bazargan, "DC grid management of a multi-terminal HVDC transmission system for large offshore wind farms," in *Sustainable Power Generation and Supply, 2009. SUPERGEN '09. International Conference on*, 2009, pp. 1-7.